Available online at www.sciencedirect.com
ScienceDirect
Cement & Concrete Composites 30 (2008) 347–352
Cement & Concrete Composites
www.elsevier.com/locate/cemconcomp

Composite cement of magnesium-bearing phosphoaluminate–hydroxyapatite reinforced by treated raw silk fiber

Shiqun Li [a,*], Biao Liu [a], Jiping Cheng [b], Jiashan Hu [a]

[a] School of Materials Science and Engineering, Jinan University, 250022 Shandong, Jinan, People's Republic of China
[b] 129 A, Materials Research Laboratory, The Pennsylvania State University, University Park, PA 16802, USA

Received 21 August 2006; received in revised form 15 June 2007; accepted 6 August 2007
Available online 23 August 2007

Abstract

Hydraulic hardened paste of magnesium-bearing phosphoaluminate–hydroxyapatite composite cement (MPAHC) reinforced by 0.5 wt.% addition of raw silk possesses splitting strength of 14.9 ± 0.2 MPa and Vickers micro-hardness of 2.22 GPa, which are increased by 22.2% and 42.3%, respectively, in comparison with that of the control ones after curing for 24 h at 37 °C. X-ray linear scanning analysis and FT-IR spectra suggest that the chemical bonds might have been developed at the interface between the treated raw silk and the hydrates in MPAHC hardened pastes.

Keywords: Composite cement of magnesium-bearing phosphoaluminate–hydroxyapatite; Treated raw silk; Mechanical properties

1. Introduction

Various kinds of bio-ceramics and polymers have been developed and widely used in the fields of osteo-, orthopaedic and dental surgery, etc. [1–3]. Ceramic materials are very inconvenient in service due to the poor readiness of shaping; polymers [4,5] are poor in durability due to they possess no hydraulicity and can only harden by acid-basic reaction. However, hydraulic bio-cements, for instances: calcium phosphate cement (CPC) [6] and zinc phosphate cement [7], show many advantages in comparison with ceramics, polymers and some other materials owing to they are easy to shape, injectable, and can be maintained locally; but the brittle behavior and poor mechanical properties of hydraulic bio-cements limit their use in loaded conditions, and the vivo resorption is also very slow. A new way to produce macropores in CPC by adding $NaHCO_3$ to enhance the resorption, but 85% decrease of the compressive strength has been noted [8].

Fibers have been employed as reinforcing materials, such as carbon fiber [9] or ceramic fiber [10], but they are poor in bio-compatibility. A new idea to employ treated raw silk for reinforcing this kind of materials has been put forward by the authors. Raw silk is composed of silk fibroin (70–75%), silk sericin albumen (20–25%), wax (0.45–0.8%), carbohydrates (1.2–1.6%) and inorganic ingredients (~0.7%). Due to the strong interaction between the covalent chemical bonds along its axis orientation and the existence of non-crystalline region within the polypeptide-chain structure, raw silk possesses excellent high tensile strength of 10 GPa and high fracture absorbing energy which is even stronger than that of Kevlar (a kind of aromatic polyamide fiber) and steel [11]. In addition to treated silk fiber, the selected material for this study is magnesium-bearing phosphoaluminate–hydroxyapatite cementitious material. Since Ca-aluminate based bio-cement exhibits very low clotting behavior and can maintain high platelet count number, but the high amount of $[AlO_4]$ group introduced may be harmful to the human body; on the contrary, CPC exhibits high clotting behavior and shows low platelet count although they possesses high biocompatibility [12]. Phosphoaluminate cement created by

* Corresponding author. Tel.: +86 531 82765853/7027; fax: +86 531 87974453.
E-mail address: mse_lisq@ujn.edu.cn (S. Li).

0958-9465/$ - see front matter © 2007 Elsevier Ltd. All rights reserved.
doi:10.1016/j.cemconcomp.2007.08.009

the authors [13] might be the preferential candidate for biocement purpose. To obtain desirable hydraulicity and in parallel to maintain high biocompatibility, magnesium oxide and hydroxyapatite have been employed in the system studied, and the novel idea to enhance the mechanical strength of this system by treated raw silk has been studied here.

2. Experimental

2.1. Starting materials

Starting materials were prepared by sol gel process shown schematically in Fig. 1. The following reagent chemicals were selected in this study: $Ca(NO_3)_2 \cdot 4H_2O$, H_3PO_4, $Al(NO_3)_3 \cdot 9H_2O$ and $Mg_3(PO_4)_2 \cdot 8H_2O$ (Beijing Red Star Chemical Plant), and silica sol (Qing Dao Marine Chemical Plant).

2.2. The design of phase composition of MPAHC clinker

MPAHC clinker was made up of the clinker of magnesium-bearing phosphoaluminate cement and the clinker of hydroxyapatite. The clinker of magnesium-bearing phosphoaluminate cement was formed by proportioning the starting materials with the molar ratio of $(CaO + MgO)/(Al_2O_3 + P_2O_5 + SiO_2) = 1.94$ and $CaO/P_2O_5 = 2.05$ firstly, then sintering the material at the temperature of 1380 °C for 30 min, hereafter, quenching the material at RT (room temperature). The clinker of magnesium-bearing phosphoaluminate cement obtained is mainly composed of novel calcium phosphoaluminate solid solution (abbreviation LH_{ss}, XRD *d*-space: 0.375, 0.262, 0.215 and 0.288 nm) [13], calcium phosphate, magnesium phosphate and calcium aluminate solid solution. The clinker of poor crystalline hydroxyapatite was synthesized by proportioning the starting material according to the formula of $Ca_5(PO_4)_3OH$, then burning it at 1300 °C foe 30 min, and then quenching at RT.

2.3. Raw silk surface treatment

Fig. 2 shows the section (a) and the structure (b) of a silk. Raw silk was soaked into nitric acid (1:10) for 2 h at RT, thereafter, was rinsed by tap water thoroughly, then, was fresh soaked into the solution of alcohol:ethanol = 1:1 for 10 h at room temperature, and then the fiber was dried at about 60 °C for 3 h, after cooling the treated silk was cut into the length of 2 mm for the use of experiment.

2.4. Preparation of specimens

MPAHC consists of magnesium-bearing phosphoaluminate clinker and hydroxyapatite in the proportion of 75:25 in weight percent. The mix was powdered with proper amount of superplastcizer to the particle size smaller than 35 μm, in which, about 70.0 w/% of the particles were concentrated in range of the size smaller than 7.9 μm as shown in Fig. 3. If the fineness of a cement powder is high, the reactivity and the hydraulicity will be high when the powder reacts with water due to the high specific surface area. The hydration specimens with the size of 12 mm in diameter and 6 mm in thickness were prepared by mixing the cement and treated raw silk intimately at the water/solid ratio of 0.15, then molding it. The pastes were set in 6–10 min and hardened in about 15 min at RT, hereafter, the specimens were demolded and cured in distilled water at 37 °C for 24 h, and then were measured for tensile splitting strength and Vickers micro-hardness. The fraction of treated raw silk was in the range of 0.2–0.8 wt.% while taking the specimen with the 0.0 wt.% of treated raw silk as a control.

2.5. Evaluation methods

Particle size distribution analysis of powdered MPAHC was conducted by Laser Diffraction Particle Size Analyzer LS 13 320 (BECKMAN COULTER) with 220 V and 56 Hz in the size range of 0.04–2000 μm for 90 s at RT. Fig. 4 shows schematically the determination of splitting

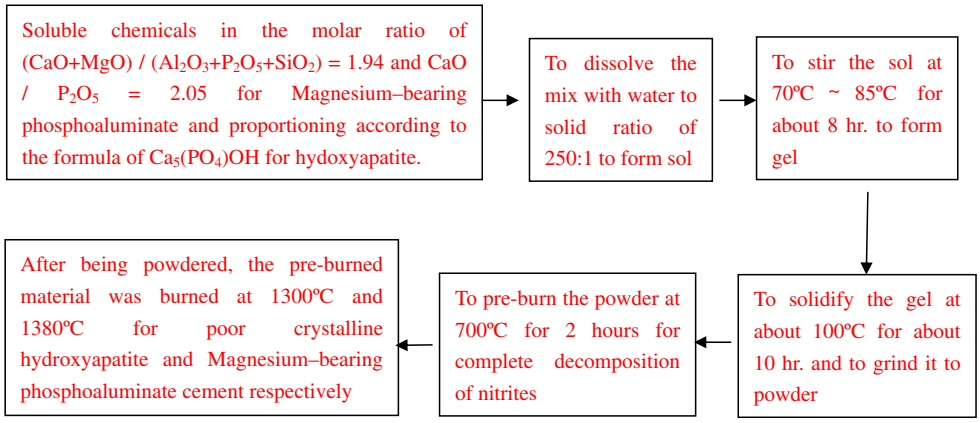

Fig. 1. Schematic routing of sol–gel process for the preparation of starting materials.

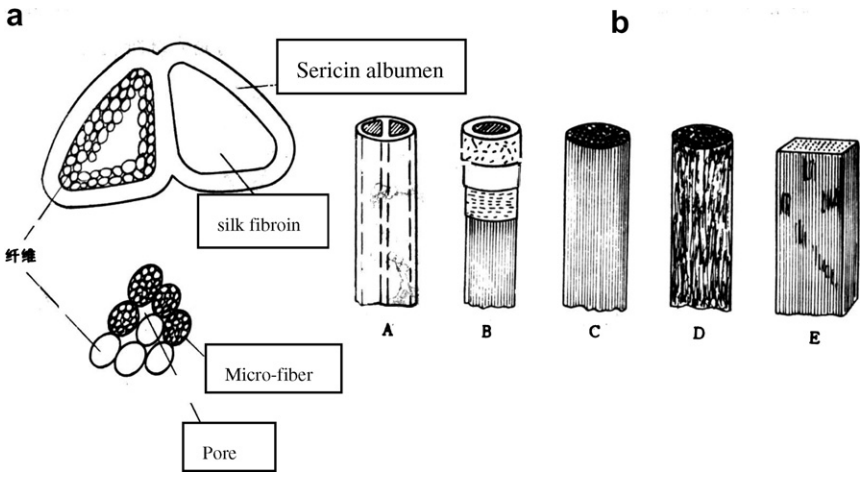

Fig. 2. The section (a) and the structure (b) of a silk: (A) a silk is composed of two pieces of fibroin; (B) a piece of fibroin embodied by sericin albumen; (C) a piece of fibroin is composed of 90–1400 pieces of fibers with the diameter of 0.2–0.4 μm; (D) a piece of fiber consists of 800–900 micro-fibers with the diameter of about 10 nm; (E) the structure of alternating crystal region with non-crystal region.

strength under the loading rate of 1 kN/s, and Fig. 5 shows the testing scheme of Vickers micro-hardness on the loading stress of 2.66×10^{-2} MPa for 20 s. Infrared spectroscopy analysis (IR) was performed by the instrument of FTS-165, Bio-Rad, USA; the resolution and accuracy of the instrument were 0.17 cm^{-1} and 0.01 cm^{-1}, respectively. SEM (S-2500, Japan, HITACHI) with X-ray energy-dispersing analysis (England, VG Scientific Instrument Company) was employed for morphology observation and the evaluation of the interface between cement hydrates and the treated silk fiber.

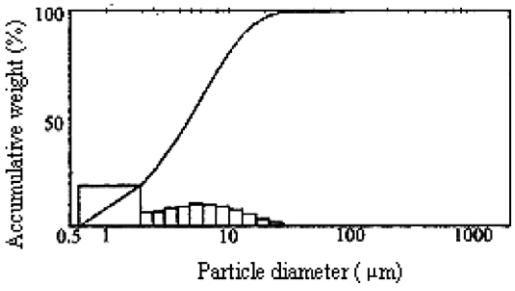

Fig. 3. Particle size distribution of powdered MPAHC, showing that about 71.1 wt.% of the particles are concentrated at the size range of smaller than 7.9 μm.

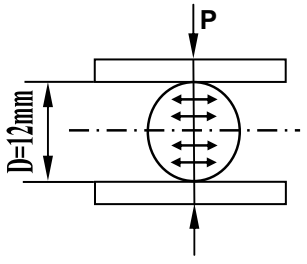

Fig. 4. Sketch of testing for splitting strength.

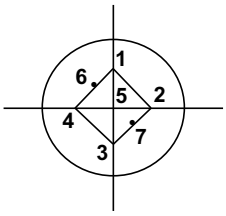

Fig. 5. Schematic distribution of testing points for splitting strength.

3. Results and discussion

Figs. 6 and 7 show the dependence of mechanical properties on the fraction of treated raw silk. Each value of splitting strength is the average of six specimens, the error is in the range of ±0.2 to ±0.6; each value of Vickers micro-hardness (VH) is the average of 42 testing dots of six specimens, the error is in the range of ±0.02 to ±0.07. Fig. 6 shows that the splitting strength of hardened paste

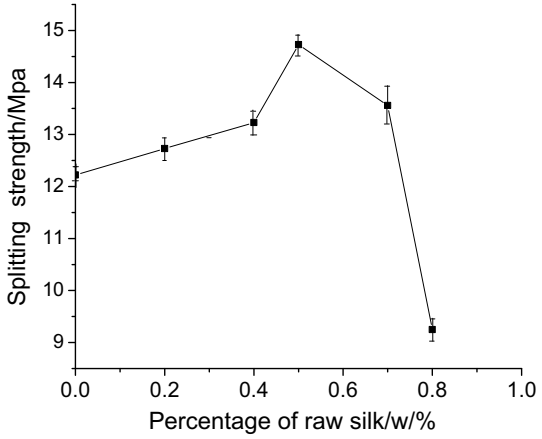

Fig. 6. The dependence of splitting strength of hardened pastes on the fraction of raw silk, which are cured at 37 °C for 24 h. Each point is the average of the minimum and maximum testing values of six specimens, the error is in the range of ±0.2 to ±0.6.

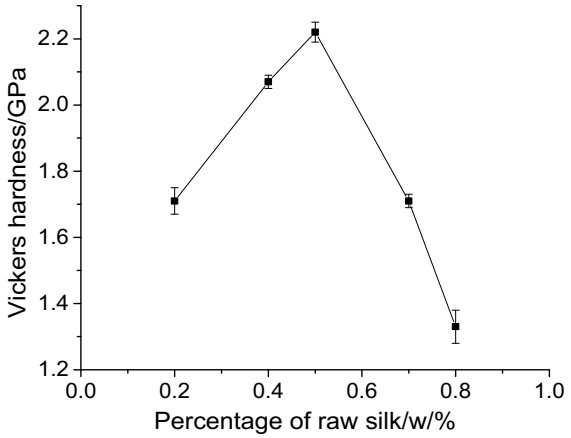

Fig. 7. The dependence of Vickers hardness of hardened pastes on the fraction of raw silk, which are cured at 37 °C for 24 h. Each point is the average of the minimum and maximum testing values of 42 points, the error is in the range of ±0.02 to ±0.07.

with 0.5 wt.% fiber is 14.9 ± 0.2 MPa, it is enhanced by 22.2% in comparison to 12.2 MPa of the control one; Fig. 7 shows that VH of the hardened paste with 0.5 wt.% silk is 2.22 GPa, it is increased by 42.3% as compared with 1.56 GPa of the control one. The remark decline of the mechanical properties of hardened pastes with the fiber amount higher than 0.5 wt.% is caused by the present of fiber cluster in pastes. It is very difficult to disperse the fiber if its amount is high. Thanks to the desirable particle size distribution and the fineness, to the intrinsically high mechanical property of treated raw silk itself and to the chemically bonded interfaces formed between the hydrates and the silk in hardened pastes, which give rise to the high mechanical properties of MPAHC hardened pastes, in which the surface treatment of the silk is a key technique that is responsible for the chemical bond. Fig. 8a shows the SEM morphology of raw silk after surface treatment. There are some sericin albumen attachments on the surface of the fiber; X-ray energy-dispersing spectrum (England, VG Scientific Instrument company, specimen was coated with gold, Au) in Fig. 8b shows the main elements composition of the raw silk is carbon, oxygen, nitrogen and hydrogen (not present by this technique here) that make up of the dominant groups of carboxyl and amino as shown in IR spectrum (c) of Fig. 11. It is these groups, especially carboxyl group, to favor the bond between MPAHC hydrates and silk. SEM morphology of Fig. 9a shows the intimated bond of these two materials and Fig. 9b shows the element composition at point 1 in Fig. 9a. The elements presented right at the location of interface are Ca, P, Si, Mg, O, N and C. Fig. 10 shows X-ray linear scanning at the interface region of 13.2 μm marked in Fig. 9a. It exhibits that there are not only elements of Al and P presented originally in cement paste but also element C presented originally in the silk at the interface, and the concentration of these elements alter gradually instead of abruptly. The concentration of element C declines from interface to cement paste and so do that of elements Al and P from interface to silk. It might imply the high inter-diffusing of elements and the present of chemical bonds at the vicinity of the interface. FT-IR spectra shown in Fig. 11 confirm this deduction further. In comparison the spectrum (b) with (a) and (c) respectively, it can be seen that: (1) Eight bands originally presented in the spectrum (c) of raw silk fiber are absent in spectrum (b) of MPAHC hardened paste with 0.5 wt.% silk fiber. The relatively sharp eight bands are: the band of groups N–H and OH at around 3421.73 cm^{-1}, band of C–H at 1385.04 cm^{-1}, O=C at 1700.54 cm^{-1}, –C–N at 1048.47 cm^{-1} and 1234.53 cm^{-1}, OH in carboxyl group at 965.13 cm^{-1}, and bands of –O–NO group at 619.81 cm^{-1} and 697.59 cm^{-1}; (2) A double stretching vibration adsorption band of group OH^- [14] at 3399.86 cm^{-1} and 3254.31 cm^{-1} in spectrum (a) of MPAHC hardened control paste transforms into a shoulder band at 3432.33 cm^{-1} in spectrum (b), which shifts to high wavenumber by 32.47 cm^{-1}, consequently, the bond

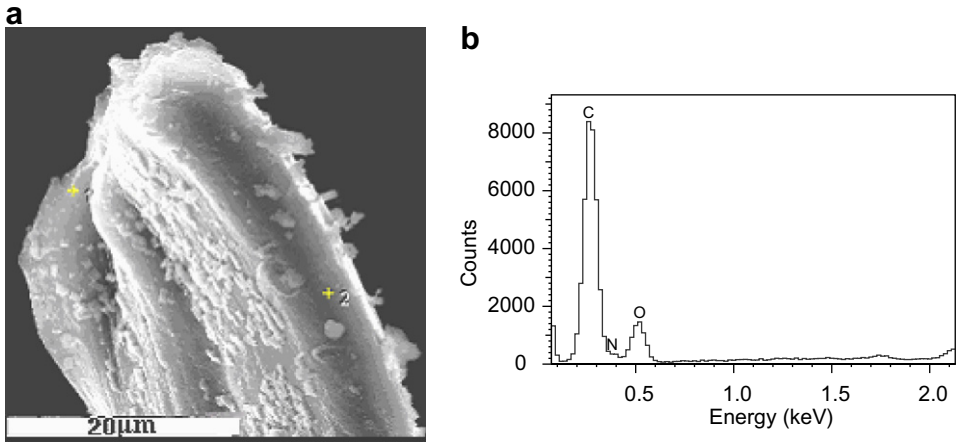

Fig. 8. SEM morphology of treated raw silk (a) demonstrates that there are some sericin albumen attachments on the surface of the fiber. X-ray energy-dispersing spectrum (b) shows that the element composition of raw silk is mainly the elements of carbon, oxygen and nitrogen.

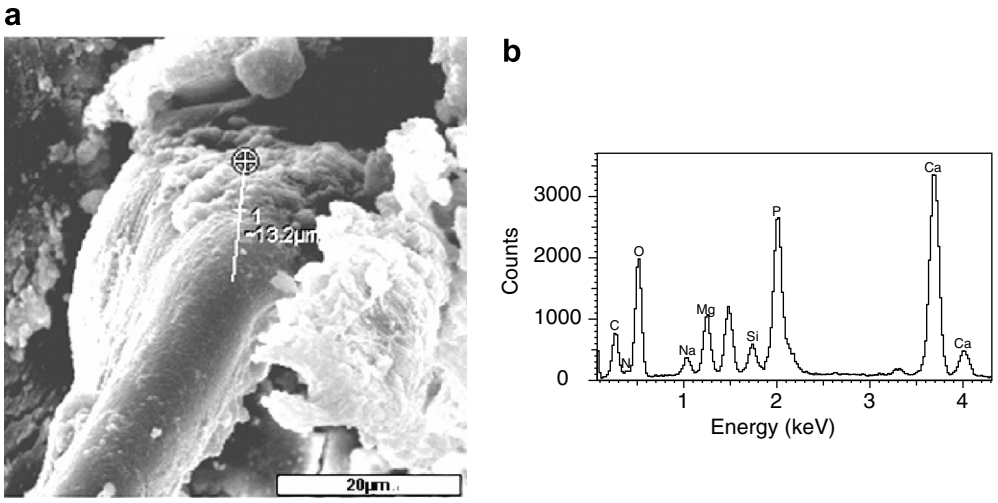

Fig. 9. SEM morphology of hydrated paste (a) showing that the silk fiber embeds into the hydrates. The X-ray energy-dispersing spectrum (b) shows the element composition at point 1 in Fig. 6a.

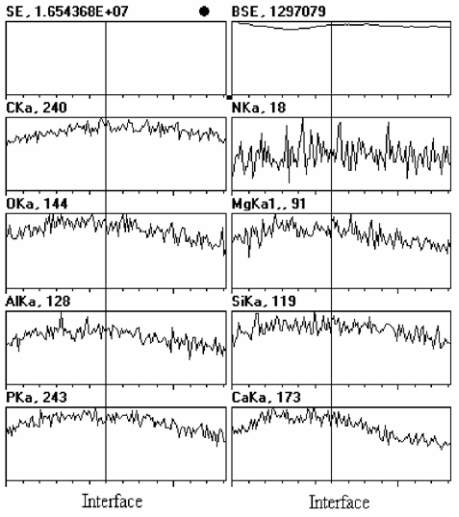

Fig. 10. X-ray linear scanning shows the distribution of element concentration at the interface between hydrates and silk at the location marked in Fig. 6a.

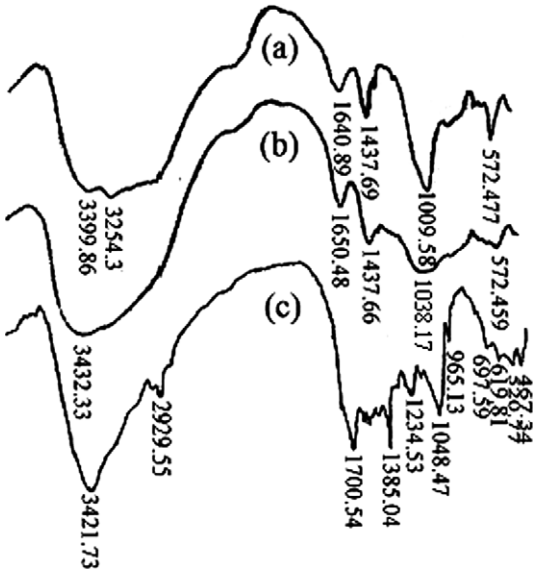

Fig. 11. FT-IR spectra: (a) control MPAHC hardened paste; (b) MPAHC hardened paste with 0.5% treated silk fiber and (c) treated raw silk fiber.

energy is increased by 388.67 J in MPAHC; in parallel, the band shape widens and its intensity increases, which suggest that the poly-groups of $[OH^-]_n$ and hydrogen bond between molecules occur, and the concentration of hydroxyl increases which is a prerequisite for a material whether or not possesses biocompatibility. (3) The asymmetry stretching vibration band of P–O group at 1009.58 cm^{-1} broadens pronouncedly from spectrum (a) to (b), which might suggests the formation of some poly-groups of $[PO_4]_n$. (4) Carboxyl band at 1437.69 cm^{-1} becomes weak and presents shoulder splitting, in consideration the increase of the intensity and the shiftiness of band of group OH^-, it might imply the substitution of group hydroxyl for carboxyl in the lattice of MPAHC hydrates. (5) The band of 572.477 becomes less infrared activity and shifts gently toward the low wavenumber.

The above considerations suggest that the chemical bonds might formed between groups of $[PO_4]$, $[AlO_4]$ and OH in MPAHC hydrates and groups of carboxyl group, O═C, –C–N and –O–NO in silk fiber at the interface, which is the intrinsic factor to strengthen and toughen MPAHC composite hardened pastes, and that MPAHC composite might possesses high bio-compatibility due to the high concentration of hydroxyl group.

4. Conclusion

1. Hydraulic MPAHC composite hardened paste containing treated raw silk of 0.5 wt.% possesses the splitting strength of 14.9 ± 0.2 MPa and Vickers micro-hardness of 2.22 GPa, which are increased by 22.2% and 42.3%,

respectively, in comparison with that of the control one after curing at 37 °C for 24 h.

2. The high mechanical performances of hydraulic MPAHC are given by the combination of high and early strength PALC employed here, the desirable particle size distribution of MPAHC and the treated raw silk.
3. The chemical bonds might have been developed at the interface between cement hydrates and treated raw silk and the formation of poly-groups of $[OH^-]_n$ and $[PO_4]_n$ in MPAHC paste reveal the intrinsic factor of strengthening and toughening the hardened pastes of MPAHC composite cement.

Acknowledgements

The author would like to thank the National Nature Science Foundation of China (50572035) and the Shandong Province Nature Science foundation of China (Q2003.F02) for the financial support of this study.

References

[1] Wang Jinmei, Yao Songnian. The progress and prospect on the study of biomaterials and its bionics. J Mater Res 2000;14(4):337–42 [in Chinese].
[2] Choi Je Won, Kong Young Min, Kim Hyoun Ee. Reinforcement of hydroxyapatite bioceramic by addition of Al_2O_3 and Ni_3Al. J Am Ceram Soc 1998;81(7):1743–8.
[3] Cu Chenglin, Zhu Jjinchuan. The progress on the study of apatite-based bio-composite. J Mater Guidance 1999;13(2):51–4 [in Chinese].
[4] Jasper LE, Deramond H, Mathis JM, Bellkoff SM. Materials properties of various cements for use with vertebroplasty. J Mater Sci – Mater Med 2002;13:1–5.
[5] Kenny SM, Buggy M. Bone cements and fillers: a review. J Mater Sci – Mater Med 2003;14:923–38.
[6] Brown WE, Chow LC. US Patent 451840, October 20, 1985.
[7] Steinke R, Newcomer P, Komarneni S, Roy R. Dental cements: investigation of chemical bonding. Mater Res Bull 1988;23(1):13–22.
[8] del Real RP, Wolke JGC, Vallet-Regi M, Jansen JA. A new method to produce macropores in calcium phosphate cements. Biomaterials 2002;23:3673–80.
[9] Reda Taha MM, Shrive NG. Enhancing fracture toughness of high performance carbon fiber cement composites. ACI Mater J 2001; 98(2):168–78.
[10] Ma Yiping, Zhu Beirong. Properties of ceramic fiber reinforced cement composites. Cem Concr Res 2005;35:296–300.
[11] Cui Fuzhai, Feng Qingling. Biomaterials science. Beijing: Science Press; 1996 [chapter 2, in Chinese] p. 23–6.
[12] Axén N, Ahnfelt N-O, Persson T, Hermansson L, Sanchez J, Larsson R. A comparative evaluation of orthopaedic cements in human whole blood. Ceram Eng Sci Proc 2005;26(6):71–7. Biomaterials, performance and testing. In: Mizuno Mineo, editor, Zhu Dongming, Kriven Waltraud M, General editors. Proceedings of the 29th international conference on advanced ceramics and composites – advances in bioceramics and biocomposites.
[13] Li Shiqun, Hu Jiashan, Liu Biao, et al. Fundamental study on phosphoaluminate cement. Cem Concr Res 1999;29(10):1549–54.
[14] Zhong Haiqing. Elementary infrared spectroscopy. Beijing: Chemistry Industry Press; 1983. p. 113–32 [chapter 5, in Chinese].